Cooperativity and Specificity in the Interactions between DNA and the Glucocorticoid Receptor DNA-Binding Domain†

Torleif Härd,*,‡ Karin Dahlman,§ Jan Carlstedt-Duke,§ Jan-Åke Gustafsson,§ and Rudolf Rigler‡

Department of Medical Biophysics, Karolinska Institute, Box 60400, S-104 01 Stockholm, Sweden, and Department of Medical Nutrition and Center for Biotechnology, Karolinska Institute, Huddinge University Hospital, S-141 86 Huddinge, Sweden

Received November 1, 1989; Revised Manuscript Received January 24, 1990

ABSTRACT: We have employed fluorescence spectroscopy to study the chemical equilibrium between a 115 amino acid protein fragment containing the DNA-binding domain of the human glucocorticoid receptor (DBDr) and a 24-base-pair DNA oligomer containing the glucocorticoid response element (GRE) from the mouse mammary tumor virus promoter region and compared it with the binding to nonspecific DNA at various ionic conditions. We find that binding to both DNAs is cooperative but that DBDr shows a higher affinity for the GRE than for nonspecific DNA and that this difference is more pronounced at increased salt concentrations. Sequence-specific binding to the GRE sequence at 570 mM monovalent cations can be described by a two-site cooperative model, and this supports the notion that DBDr binding to the GRE is enhanced by dimer formation at the recognition site. The product between the (average) association constant for binding to a GRE half-site and the cooperativity parameter was estimated to be $K\omega = (1-4) \times 10^7$ M^{-1} at this salt concentration and 20 °C. The sequence-specific binding is not very sensitive to salt concentration in the interval 270–570 mM monovalent cations. However, at lower salt (70 mM) additional binding takes place, presumably nonspecific (cooperative) association to DNA adjacent to the GRE sequence. DBDr binding to nonspecific DNA can be described by the McGhee–von Hippel model for cooperative binding to a chain polymer and is very sensitive to ionic conditions. The nonspecific binding is only about 5 times weaker than specific binding to the GRE sequence at 70 mM salt, but more than 2 orders of magnitude weaker at 570 mM. The equilibrium data are also discussed in view of what is known about the binding of the native glucocorticoid receptor complex.

Considerable interest has recently been focused on the interactions between DNA-binding steroid hormone receptors and their DNA response elements (Yamamoto, 1985; Evans, 1988; Beato, 1989, and references therein). The sequence-specific DNA-binding activity of the glucocorticoid receptor is localized to a distinct domain (comprising amino acids 394–498 of the human glucocorticoid receptor) (Carlstedt-Duke et al., 1987) that shows a high degree of sequence homology with corresponding domains in other steroid receptors (Evans, 1988; Beato, 1989). Protein fragments containing the DNA-binding domain of the receptor expressed in *Escherichia coli* exhibit sequence-specific binding to the glucocorticoid receptor response element (GRE)[1] (Freedman et al., 1988; Dahlman et al., 1989). These protein fragments contain two Zn atoms, which are required for proper folding and DNA binding (Freedman et al., 1988; Carlstedt-Duke et al., 1989). In fact, all members of this family of hormone receptors contain two putative Zn-binding regions (Evans 1988; Freedman et al., 1988; Beato, 1989; Berg, 1989) that are reminiscent of the so-called "Zn fingers" of TFIIIA (Miller et al., 1985). The two Zn-binding regions of the steroid receptors are, however, not identical with the Zn fingers of TFIIIA, indicating that the steroid/thyroid receptors represent a novel structural motif for DNA binding and recognition (Berg, 1989).

It has been demonstrated that the DNA-binding domain of the human glucocorticoid receptor expressed in *E. coli* (DBDr) binds cooperatively to two sites on the GRE (Tsai et al., 1988) suggesting that protein–protein interactions might be important in the recognition process. The notion of protein–protein interactions within the glucocorticoid receptor is also supported by recent studies suggesting that the activated (DNA-binding) receptor forms oligomers in the free state and also binds DNA as a dimer (Wrange et al., 1989).

These observations have motivated us to undertake a more detailed investigation of the DBDr–DNA equilibrium with the objective of obtaining quantitative information about association constants and cooperativity parameters. In this paper we report on the chemical equilibrium between specific as well as nonspecific DNA and the 115 amino acid DBDr fragment at various salt concentrations. The fluorescence from four tyrosines in the protein is quenched upon binding to DNA, thus providing a suitable probe for monitoring the DBDr–DNA equilibrium. We study the sequence-specific binding to a 24-base-pair DNA duplex containing a GRE [footprint 1.3 from the mouse mammary tumor virus promoter region (Payvar et al., 1983)] and compare it to nonspecific binding to calf thymus DNA. In short, we find that both specific and nonspecific binding are cooperative but that the affinity for binding to the GRE sequence is higher than for binding to nonspecific DNA and that nonspecific binding is further

† This work was supported by grants from the Swedish Medical Research Council (2819 to J.C.-D. and J.-Å.G.), the Swedish Natural Sciences Research Council (to R.R.), and the Swedish National Board for Technical Development. T.H. acknowledges a research fellowship from the Swedish Natural Sciences Research Council, J.C.-D. acknowledges a research fellowship from the Swedish Medical Research Council, and K.D. acknowledges a predoctoral fellowship from the Swedish Medical Research Council.

‡ Department of Medical Biophysics.

§ Department of Medical Nutrition and Center for Biotechnology.

[1] Abbreviations: DBDr, glucocorticoid receptor DNA-binding domain; bp, base pair; GRE, glucocorticoid receptor response element; TFIIIA, transcription factor IIIA; DTT, dithiothreitol; FP, footprint.

0006-2960/90/0429-5358$02.50/0 © 1990 American Chemical Society

suppressed when the salt concentration of the solution is increased. We also find that the binding of DBDr to the GRE at high salt conditions (570 mM) is described by a two-site cooperative binding model in agreement with the suggested dimeric binding.

Materials and Methods

Materials. The DNA-binding domain of the human glucocorticoid receptor (DBDr) was purified and the sequence-specific DNA-binding activity was checked as described by Dahlman et al. (1989). For these studies purified DBDr was dialyzed against 50 mM NaCl, 20 mM Tris-HCl, and 0.3 mM DTT at pH 7.5, and stock solution concentrations (5–12 μM) were determined spectrophotometrically by using the extinction coefficient ϵ_{280} = 6000 M^{-1} cm^{-1} (calculated from tyrosine absorption data). Calf thymus (CT) DNA (Sigma, Type I) was dissolved in buffer and a low degree of protein impurity was assured by an absorbance ratio $A_{260}/A_{280} \geq 1.9$. The 24-bp DNA oligomer 5′-TTTTTGGTTACAAACTGTTCT-TAA-3′ [FP1.3 (Payvar et al., 1983)] and its complementary strand were synthesized on an Applied Biosystems 380B DNA synthesizer. DNA concentrations were determined by using the extinction coefficient ϵ_{260} = 13 200 M base pairs^{-1} cm^{-1} (Mahler et al., 1964). All experiments were carried out at 20 °C in 50 mM NaCl, 20 mM Tris-HCl, and 0.3 mM DTT at pH 7.5 with various amounts of concentrated KCl added to adjust the salt concentration.

Fluorescence Measurements. Steady-state fluorescence was measured on a Shimadzu RF540 spectrofluorometer with excitation and emission wavelengths set at 280 and 307 nm, respectively, corresponding to absorption and emission maxima of the four tyrosines in DBDr. The measured intensity was corrected for background emission and Raman light scattering from water by subtracting signals from blank buffer or DNA + buffer samples. Fluorescence intensities at high DBDr or DNA concentrations were also corrected for "optical filtering" effects. Equilibrium titrations were performed either as "forward" titrations, where protein was added to a constant DNA concentration, or as "reverse" titrations, where DNA was added to a constant protein concentration.

Analysis of Fluorescence Data. The concentrations of free and bound DBDr at various points during the fluorescence titrations were calculated from the observed fluorescence quenching $Q_{obs} = (I_0 - I)/I_0$, where I is the observed (protein) fluorescence in the presence of DNA and I_0 is the fluorescence intensity in the absence of DNA. The concentration of DBDr bound to DNA was determined by using $C_{bound} = (Q_{obs}/Q_{max})C_{tot}$, where C_{tot} is the total DBDr concentration of the sample and Q_{max} is the maximum fractional quenching, i.e., the quenching that would be observed if all the protein in the sample was bound to DNA. Values of Q_{max} for DBDr in complexes with CT DNA and the GRE 24mer were determined from reverse titrations (Figure 2), where a large excess of DNA could be added to make the binding quantitative.

It is important to note that the above method of calculating the concentration of bound protein would not be justified if different binding modes result in different fluoresecence quantum yields. For instance, proteins bound to isolated DNA sites might have a fluorescence quantum yield that differs from that of proteins that are (cooperatively) bound to contiguous sites. A method to resolve this matter has been described by Bujalowski and Lohman (1987), who showed that an unambiguous evaluation of DNA–protein equilibria can be obtained from several reverse titrations performed at various protein concentrations. For DBDr binding to the GRE 24mer at 270 mM salt, we find that binding isotherms constructed by the Bujalowski–Lohman method coincide with binding isotherms obtained using the (simpler) method described above (Figure 4), indicating that Q_{max} is not a function of the extent of protein–protein interactions in the bound state, and we assume that this also holds for cooperative binding to CT DNA.

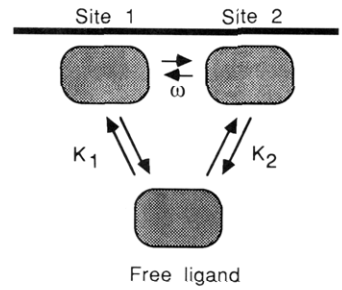

FIGURE 1: Two-site model for binding of DBDr to the GRE at high salt concentrations. K_1 and K_2 are association constants for binding to sites 1 and 2, respectively, and ω is the cooperativity parameter. The Scatchard expression for the expected binding isotherm for this model (derived in the Appendix) is given by eq 2.

Analysis of Binding Isotherms. Binding isotherms are presented as Scatchard plots with $r/[L]$ plotted against r (Cantor & Schimmel, 1980), where r is the ratio of bound protein ligands per DNA base pair (in the case of nonspecific binding to high molecular weight CT DNA) or bound ligands per 24mer DNA fragment (r') and [L] is the free ligand concentration. DBDr binding to high molecular weight CT DNA is analyzed in terms of the McGhee–von Hippel model for cooperative binding to a chain polymer (McGhee & von Hippel, 1974):

$$r/[L] = K(1 - nr)\left[\frac{(2\omega - 1)(1 - nr) + r - R}{2(\omega - 1)(1 - nr)}\right]^{n-1} \times \left[\frac{1 - (n + 1)r + R)}{2(1 - nr)}\right]^2 \quad (1)$$

with

$$R = \{[1 - (n + 1)r]^2 + 4\omega r(1 - nr)\}^{1/2}$$

where K is the intrinsic binding constant in M^{-1}, n is the number of DNA base pairs covered by one ligand, and ω is the cooperativity parameter ($\omega > 1$ for cooperative binding).

DBDr binding to the GRE 24mer is not accurately described by the McGhee–von Hippel model because this DNA is too short. However, at high salt concentrations we find that Scatchard plots of DBDr binding to the GRE 24mer extrapolates to a maximum binding ratio of 2 bound proteins/GRE 24mer (as described below and shown in Figure 4). This equilibrium was therefore modeled by using the scheme shown in Figure 1. If we assume that the intrinsic binding constants for binding to the two sites are K_1 and K_2, respectively, and that the cooperativity parameter for binding to the second site when the first site is already occupied (or vice versa) is ω, then the binding isotherm can be written in the Scatchard form as (see Appendix)

$$r'/[L] = \{K_1 + K_2 + [(K_1 + K_2)(r' - 1) + R']/(2 - r')\}/\{1 + (K_1 + K_2)[(K_1 + K_2)(r' - 1) + R']/2\omega K_1K_2(2 - r') + [(K_1 + K_2)(r' - 1) + R']^2/4\omega K_1K_2(2 - r')^2\} \quad (2)$$

with

$$R' = [(K_1 + K_2)^2(r' - 1)^2 - 4r\omega K_1K_2(r' - 2)]^{1/2}$$

where r' is the ratio of bound DBDr to GRE 24mer. Nonlinear least-squares fits of equilibrium data to eqs 1 and 2 were

Table I: Best-Fit Parameters for the DBDr–DNA Equilibrium

DNA	salt concn[a] (mM)	model	K (M^{-1})	ω	n (bp)
CT DNA	70	McGhee–von Hippel	2.4×10^4	51	12.5
	145	McGhee–von Hippel	5.8×10^3	168	31
	320	*b*			
GRE 24mer	70	*c*	$\sim 2 \times 10^6$ [d]		
	570	two-site[e]	2.7×10^4	1.5×10^3	
			1.0×10^5 (fixed)	108	

[a] Including 20 mM Tris-HCl, 50 mM NaCl, and varying amounts of KCl. [b] No binding detected at micromolar DNA and protein concentrations. [c] A quantitative analysis is not possible in this case, as discussed in the text, and only an approximate estimate of the association constant can be obtained. [d] Value shown is M DNA fragments^{-1}, corresponding to $\sim 10^5$ M bp^{-1}. [e] Fits to eq 2 assuming $K_1 = K_2 = K$. In the first fit both K and ω are treated as variables, whereas in the second fit K is kept fixed and only ω is fitted. The two evaluations seem to fit the data equally well (Figure 4). The large differences in the results of the two evaluations are due to a large correlation between ω and K, as discussed in the text. The product $K\omega$, however, is subject to a smaller uncertainty [$K\omega = (1\text{–}4) \times 10^7$ M^{-1}].

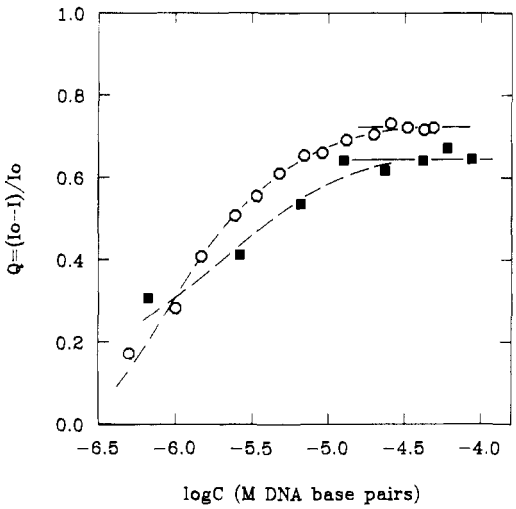

FIGURE 2: Effect of DNA concentration on DBDr fluorescence during (reverse) titrations of the GRE 24mer (○) and nonspecific CT DNA (■) at constant protein concentrations (0.5 and 0.6 μM, respectively). The ordinate shows the fractional fluorescence quenching $Q_{obs} = (I_0 - I)/I_0$, where I is the observed (protein) fluorescence in the presence of DNA and I_0 is the fluorescence intensity in the absence of DNA. Solid horizontal lines indicate estimated values of the maximum quenching, $Q_{max} = 0.72$ and 0.64 with the GRE 24mer and nonspecific CT DNA, respectively. The titrations were carried out in 20 mM Tris-HCl and 50 mM NaCl (no KCl added) at pH 7.5 and a temperature of 20 °C. Excitation and emission wavelengths were 280 and 307 nm, respectively. The data are corrected for (weak) background emission and optical filtering effects due to DNA absorption.

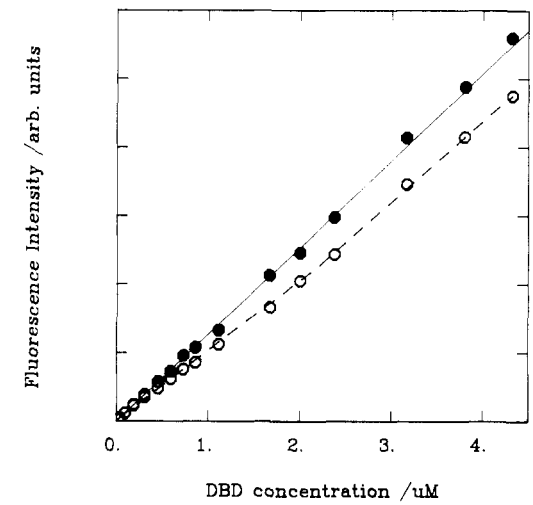

FIGURE 3: (○) Effect of DBDr concentration on the observed fluorescence intensity during a (forward) titration at constant CT DNA concentration (25 μM bp) in buffer + 75 mM KCl (total salt concentration of 145 mM). (●) Reference titration without DNA. The solid line is a linear fit to the fluorescence intensity in the absence of DNA. (The dashed line is drawn as a guide for the eye.) Experimental conditions were as in Figure 2.

carried out by using a computer program based on the Marquardt algorithm (Press et al., 1986).

Results

Fluorescence titrations of DNA at constant DBDr concentrations (reverse titrations, Figure 2) were carried out to determine the relative fluorescence quantum yield of DBDr in the bound state (Q_{max}). The observed quenching $Q_{obs} = (I_0 - I)/I_0$ increases as DNA is added, reflecting increasing amounts of bound protein, and levels off ($Q_{obs} = Q_{max}$) at high DNA concentrations when all the protein in the sample is bound to DNA. The fluorescence quantum yield in the bound state differs somewhat between DBDr complexes with CT DNA ($Q_{max} = 0.64$) and the 24mer containing the GRE ($Q_{max} = 0.72$), possibly owing to different binding modes for specific and nonspecific binding. The maximum quenching was found in both cases to be independent of ionic conditions (not shown).

Figure 3 shows the result of a typical (forward) titration of DBDr at constant DNA concentration (nonspecific CT DNA at 145 mM salt). The reference titration (no DNA) shows a linear dependence of the fluorescence intensity on DBDr concentration, as expected. The titration curve in the presence of DNA displays a sigmoidal feature that is typical of cooperative binding (Schwartz & Watanabe, 1983): At low protein concentrations the fluorescence intensity closely resembles that in the absence of DNA, indicating little or no binding. At higher protein concentrations the fluorescence intensity begins to deviate from that observed in the absence of DNA as cooperative binding takes place. At even higher concentrations the slope of the titration curve again resembles that of the reference titration, indicating saturation of available binding sites.

Scatchard plots for DBDr binding to the GRE 24mer and nonspecific CT DNA obtained from titrations at various salt concentrations are shown in Figures 4–7, and corresponding best-fit equilibrium parameters are listed in Table I. Scatchard plots for DBDr binding to the GRE 24mer at high salt (270–570 mM) are shown in Figure 4. The binding displays a pronounced cooperativity as evident from the convex shape of the plots, and the data at higher binding ratios extrapolate to a maximum binding density of 2 protein molecules/DNA fragment. Both these observations are in accordance with the notion that DBDr binds to the GRE as a dimer. It is also possible to obtain good fits of the two-site model (eq 2) to experimental data (at 570 mM salt) assuming that $K_1 = K_2 = K$. Unfortunately, the data are not good enough to distinguish between the binding constants for the two sites, i.e., to determine if $K_1 \neq K_2$, but attempts to fit the data assuming that one of the binding constants is much larger

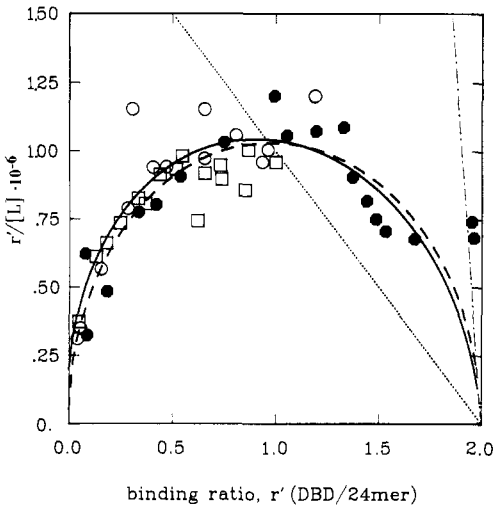

FIGURE 4: Scatchard plots for the binding of DBDr to the GRE 24mer at salt concentrations of 570 mM (●) and 270 mM (○ and □). The symbol r' denotes the ratio of bound protein molecules per GRE 24mer and [L] denotes the free ligand concentration. Data at 570 mM salt were obtained from a titration of DBDr at constant DNA concentration (0.5 μM DNA fragments), and bound and free protein concentrations were calculated from the observed fluorescence quenching as described under Materials and Methods. Data at 270 mM salt were obtained from a titration of DBDr at constant DNA concentration (0.4 μM DNA fragments) (○) as well as from several titrations of DNA at (various) constant DBDr concentrations (□) according to the method of Bujalowski and Lohman (1987). The lines represent least-squares fits of data obtained at 570 mM salt to the cooperative two-site binding model (eq 2), assuming that $K_1 = K_2 = K$. Solid line, fit of ω at $K = 10^5$ M^{-1}; dashed line, fit with both ω and K as variables. The best-fit parameters are listed in Table I. The straight lines represent the expected behavior for noncooperative binding ($\omega = 1$) with $K_1 = K_2 = 10^6$ M^{-1} (···) and $K_1 = K_2 = 10^7$ M^{-1} (---).

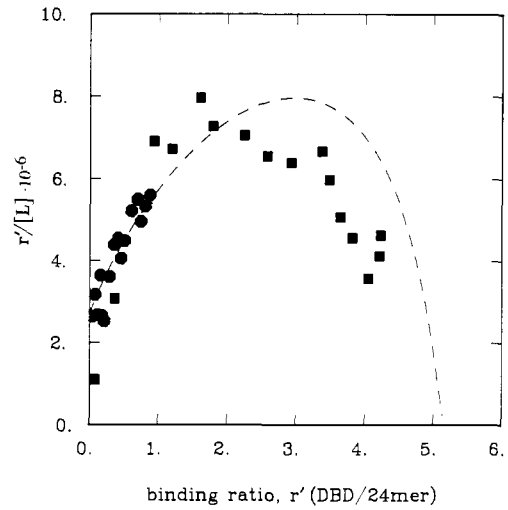

FIGURE 5: Scatchard plots for the binding of DBDr to the GRE 24mer at 70 mM salt based on titrations of DBDr at constant DNA concentrations [0.1 μM (■) and 1.6 μM (●) DNA fragments]. The dashed line represents a least-squares fit to the McGhee–von Hippel model (eq 1).

than the other ($K_1 \geq 10K_2$) were not successful, suggesting that the two binding constants are within the same order of magnitude. Neither do the fits allow accurate estimates of the association constant and cooperativity parameter to be made independently. This is because these two parameters are highly correlated in the model. As can be seen in Figure 4 and Table I, a large association constant combined with lower cooperativity seems to fit the data equally as well as a smaller association constant combined with large cooperativity. The product $K\omega$ is subject to a much smaller uncertainty and

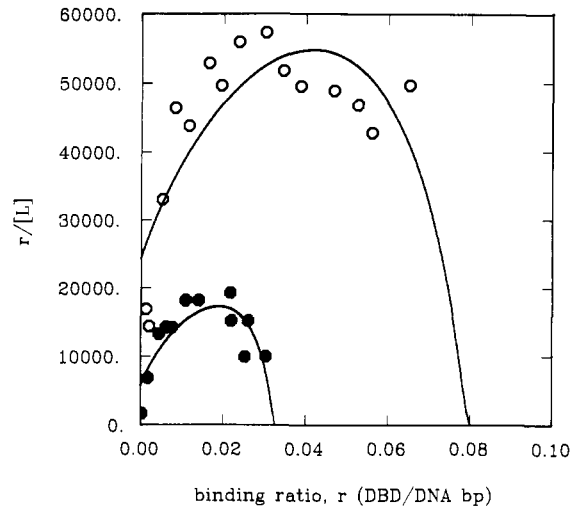

FIGURE 6: Scatchard plots for the binding of DBDr to nonspecific CT DNA at 70 mM (○) and 145 mM (●) salt based on titrations of DBDr at constant DNA concentrations (25 μM DNA bp). Note that r here denotes the ratio of bound protein molecules per DNA bp and [L] denotes the free ligand concentration. The solid lines represent least-squares fits to the MCGhee–von Hippel model. Best-fit parameters are listed in Table I.

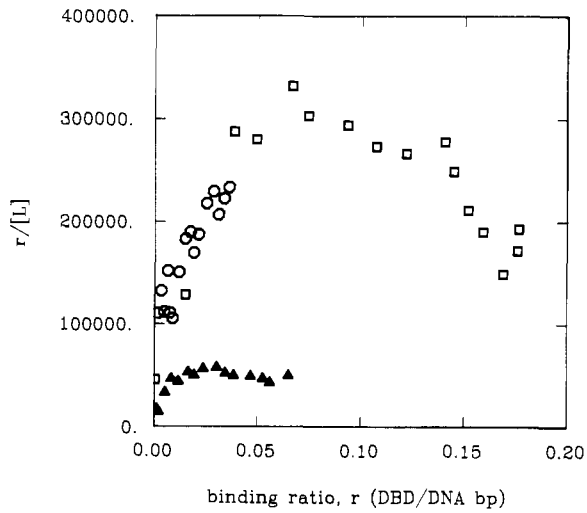

FIGURE 7: Scatchard plots for the binding of DBDr to the GRE 24mer (○ and □, same data as in Figure 5) and to nonspecific CT DNA (▲, same data as in Figure 6) at 70 mM salt (buffer with no KCl added). The data for binding to the GRE 24mer are here plotted with r = bound protein molecules per DNA bp to allow for a direct comparison of the relative binding affinities to the two DNAs (see text for details).

can be estimated to be $K\omega = (1\text{–}4) \times 10^7$ M^{-1} at this salt concentration (570 mM monovalent cations). It should be noted that the binding data obtained at 270 mM salt are very similar to those obtained at 570 mM salt, indicating that specific binding to the GRE sequence is not very sensitive to the salt concentration (Figure 4).

Figure 5 shows a Scatchard plot of DBDr binding to the GRE 24mer at 70 mM salt. This plot also shows cooperative binding, but an extrapolation of the data at high binding densities suggest that the maximum binding site density at low salt concentrations is rather high—about 4–5 bound proteins/GRE 24mer, suggesting that additional (nonspecific) binding now also takes place. The exact maximum binding density is somewhat uncertain due to the fact that the fluorescence quantum yield in the bound state differs between specific and nonspecific binding (Figure 2). The Scatchard plot in Figure 5 was calculated by assuming that $Q_{max} = 0.72$, but a calculation based on a lower value ($Q_{max} = 0.64$) does

not affect the qualitative appearance of the Scatchard plot; i.e., the maximum binding site density in this case would still be ~5 proteins/DNA fragment. We have chosen not to attempt a quantitative interpretation of both specific and nonspecific binding to a short DNA fragment, because the modeling is in this case very complicated. (The dashed line in Figure 5 is a least-squares fit of the data to the McGhee–von Hippel model showing that this model is *not* applicable in this case). However, one can still make a rough estimate of the association constant from the intercept at the abscissa—approximately 2×10^6 M 24mer fragments^{-1} (corresponding to $\sim 10^5$ M DNA bp^{-1} if one considers the 24mer as a short linear lattice).

DBDr binding to nonspecific CT DNA is also cooperative, but the binding affinity is lower than for binding to the GRE at comparable ionic conditions (Figure 6 and Table I). The affinity of the nonspecific binding mode decreases rapidly as the salt concentration increases, making accurate measurements of the amount of bound protein at >200 mM salt very difficult at the total DNA and protein concentrations used in these studies. Fits to the McGhee–von Hippel model yield binding constants on the order of $K = 6 \times 10^3$–2×10^4 M^{-1} and the cooperativity parameters on the order of $\omega = 50$–170 for nonspecific DBDr binding at 70–145 mM salt (Table I). We note that the best-fit cooperativity parameter is larger at the higher salt concentration, suggesting that increasing salt concentrations favor the protein–protein association process. However, the two parameters K and ω are, as in the two-site model, correlated in the sense that a lower value of K might be compensated by a higher value of ω and the apparent difference in cooperativity between the two salt concentrations ($\omega = 51$ versus $\omega = 168$) is therefore not necessarily significant. The product $K\omega$ decreases with increasing salt concentration, indicating that electrostatic interactions are involved in the nonspecific binding (Record et al., 1976; deHaseth et al., 1977), and the decreasing affinity is further amplified by a large reduction in the number of available binding sites (n = 12.5 and 31 bp at 70 and 145 mM salt, respectively). The large effect of salt on the binding site density is not expected for purely electrostatic binding, and this point is discussed further below. We also note that the estimated binding site density at 70 mM salt (n = 12.5 bp) differs somewhat from the binding stoichiometry reported by Hagmar et al. (1989) (n = 4.5–6 bp), who used flow linear dichroism to monitor the binding of (the same) DBDr fragment at similar salt conditions. However, the concentration of free ligand was not directly determined in these experiments, and it is possible that the apparent binding site density therefore might be somewhat overestimated.

An appropriate comparison of the binding affinities for specific and nonspecific binding at low salt concentration (70 mM) can be made in Figure 7, where the data from titrations with the GRE 24mer and CT DNA are plotted with the same definition of the binding density (bound protein molecules per DNA base pair). It is obvious that the relative affinity for specific versus nonspecific sites at low salt conditions is rather low: about 4–5, as judged from the ratio of the intercepts with the $r'/[L]$ axis. A similar value is obtained if one instead chooses to compare the free ligand concentrations corresponding to the occupancy of some fraction (e.g., 50%) of all available binding sites. On the other hand, the binding site density at this salt concentration is larger with the 24mer fragment (5 proteins/24 DNA base pairs) than with CT DNA (~2 proteins/24 DNA base pairs), and possible explanations of this effect are also discussed below.

Discussion

Evidence from an earlier study suggests that the DBDr binds cooperatively to DNA and that a dimer is formed at the GRE (Tsai et al., 1988). The present study provides a quantitative evaluation of the interactions between the DNA-binding domain and the GRE and also allows for a comparison of the relative affinities for specific versus nonspecific DNA–DBDr complexes at various salt concentrations.

At high salt (570 mM monovalent cations) we find that the binding isotherm for DBDr binding to a short DNA fragment containing the GRE can be described by a two-site cooperative model. The binding affinity does not change much between 270 and 570 mM salt, whereas binding to nonspecific CT DNA is very sensitive to the salt concentration and is more than 2 orders of magnitude weaker than the specific binding at 570 mM salt. These observations suggest that the two sites in the GRE 24mer correspond to sequence-specific sites within the DNA responsive element. Our results therefore support the notion of dimer formation at the GRE. We are also able to estimate the affinity for binding to a contiguous site ($K\omega = (1$–$4) \times 10^7$ M^{-1}, where K is the "average" binding constant for the two sites) within the dimer at these salt concentrations, although the data do not allow for independent determinations of K and ω. Neither do our data allow discrimination between the two sites, i.e., determination if $K_1 \neq K_2$, although the fits indicate that the two binding constants are within the same order of magnitude. Methylation interference studies of binding to the tyrosine aminotransferase GRE sequences show that the DBDr first binds to the TGTTCT half-site of the GRE and then to the TGTACA half-site (Tsai et al., 1988). It therefore seems likely that the two high-affinity sites we observe are due to binding to the corresponding half-sites in the GRE 24mer. It is still (theoretically) possible that the two high-affinity sites observed at high salt concentration correspond to dimer binding to only one of the GRE half-sites, but this alternative is unlikely considering the size of the DBDr. The observation that one of the half-sites is preferred over the other in the GRE sequence used in the methylation interference studies seems to be somewhat contradictory to the present results ($K_1 \approx K_2$), but it is not impossible that a small difference between K_1 and K_2 might be consistent with both studies. However, it should be noted that the GRE from the tyrosine aminotransferase gene differs at two positions from the GRE employed in this study. It should also be noted that the methylation interference studies were carried out under different buffer conditions and that a different ionic strength dependence in K_1 and K_2 might result in a preference for one of the sites or equal affinity depending on ionic conditions.

At lower salt concentrations, DBDr also binds strongly to nonspecific DNA. In contrast to the sequence-specific binding, the nonspecific binding is very sensitive to the salt concentration, indicating that it might be dominated by electrostatic contributions. However, the effect of salt concentration is observed not only in the binding constant (K) or the cooperativity parameter (ω), as expected for purely electrostatic binding (Record et al., 1976), but also in the number of available binding sites (n). This effect suggests that not all nonspecific sites are equivalent, i.e., that there might be some "semispecific" sites where the protein can make one or more specific contacts stabilizing the complex at higher salt concentrations.

At the lower salt concentration conditions we also find additional binding to the GRE 24mer, probably corresponding to the (cooperative) binding to nonspecific sites adjacent to the two GRE half-sites. The difference in affinity between

specific and nonspecific binding is quite small at low salt concentrations. In fact, our data show that the intrinsic association constant for binding to the GRE 24mer at 70 mM salt is only about 5 times higher than for nonspecific binding. On the other hand, this difference might be amplified by a larger binding site density for nonspecific binding in the vicinity of the GRE as judged from the higher maximum binding density observed with the GRE 24mer compared to CT DNA (5 protein molecules/24mer versus 2 proteins/25 CT DNA bp). A possible explanation for this difference might be that initial binding to the two specific sites in the GRE facilitates binding to contiguous nonspecific sites. This might, for instance, occur by a more favorable orientation of a protein bound to a specific site with respect to protein–protein interactions with a neighboring (nonspecifically bound) protein, although other alternatives, such as cooperative changes in DNA structure or the presence of additional semispecific sites around the GRE sequence, are also possible.

The specificity and affinity of the DBDr are lower than for many other sequence-specific DNA-binding proteins. For instance, the association constant for the the *lac* repressor–operator complex is on the order of 10^9 M^{-1} at 570 mM monovalent ions and the relative affinity of the *lac* repressor for specific and nonspecific binding sites is $\approx$ 10–100 even at very low concentrations (Record et al., 1977). The small difference in DBDr binding affinity between specific and nonspecific DNA sites at low salt concentrations together with the relatively low binding constant for specific complexes at high salt concentrations implies that the protein fragment studied here does not possess the same DNA binding affinity and specificity as the complete glucocorticoid receptor. It is possible that the relative low specificity we observe in these studies is due in part to the fact that specific binding to a short fragment might be weaker than the binding to a GRE within a longer DNA sequence. However, preliminary fluorescence studies show that the binding of the native glucocorticoid receptor complex to the GRE 24mer is 1 or 2 orders of magnitude stronger than that of the DBDr (T. Härd, unpublished), and similar results are obtained when comparing the levels of binding by footprinting of the DBDr and the native receptor complex (Dahlman et al., 1989). Studies of proteolytically digested rat liver glucocorticoid receptors have shown that removal of the N-terminal domain of the receptor leads to decreased affinity of the receptor for specific versus nonspecific DNA sequences (Payvar & Wrange, 1983). It is therfore more likely that most of the weakened binding is due to the removal of parts of the receptor complex that are important in stabilizing protein–protein interactions in the bound state, as discussed by Tsai et al. (1988). The importance of protein–protein interactions in the native glucocorticoid receptor is further emphasized by a recent study showing that activated (DNA-binding) receptor complexes can form oligomers even in the absence of DNA (Wrange et al., 1989).

In spite of the somewhat weaker specific binding of the DBDr compared to the native receptor complex, it is clear that this 115 amino acid DBDr fragment possesses enough sequence specificity, at least at salt concentrations >500 mM, to be a very suitable model system for structural studies using, for instance, nuclear magnetic resonance or X-ray crystallography.

Appendix

Derivation of Eq 2. Let f_1f_2, b_1f_2, f_1b_2, and b_1b_2 denote DNA fragments without bound proteins, with a protein bound to site 1 or 2, and with two bound proteins, respectively. Given the two-site model depicted in Figure 1, the coupled equilibria can be written as

$$L + f_1f_2 \overset{K_1}{\rightleftharpoons} b_1f_2$$

$$L + f_1f_2 \overset{K_2}{\rightleftharpoons} f_1b_2$$

$$L + f_1b_2 \overset{K_1\omega}{\rightleftharpoons} b_1b_2$$

$$L + b_1f_2 \overset{K_2\omega}{\rightleftharpoons} b_1b_2$$

where L denotes a free protein ligand, K_1 and K_2 are association constants for binding to site 1 or 2, respectively, and ω is the cooperativity parameter for binding to one of the sites if the other site is already occupied. Only one of the last two equilibria has to be used to describe the state of the system as a function of the free ligand concentration ([L]). Applying the law of mass action to the first three equilibria yields

$$[b_1f_2] = K_1[L][f_1f_2] \quad \text{(A1)}$$

$$[f_1b_2] = K_2[L][f_1f_2] \quad \text{(A2)}$$

$$[b_1b_2] = K_1\omega[L][f_1b_2] = K_1K_2\omega[L]^2[f_1f_2] \quad \text{(A3)}$$

Let r' be the ratio of bound ligands per DNA fragment:

$$r' = \frac{[b_1f_2] + [f_1b_2] + 2[b_1b_2]}{[f_1f_2] + [b_1f_2] + [f_1b_2] + [b_1b_2]} \quad \text{(A4)}$$

Substitution of (A1)–(A3) in (A4) and simplification give

$$r' = \frac{(K_1 + K_2)[L] + 2\omega K_1K_2[L]^2}{1 + (K_1 + K_2)[L] + \omega K_1K_2[L]^2} \quad \text{(A5)}$$

and solving for [L] yields

$$[L] = \{(K_1 + K_2)(r' - 1) + [(K_1 + K_2)^2(r' - 1) - 4r'\omega K_1K_2(r' - 2)]^{1/2}\}/2\omega K_1K_2(2 - r') \quad \text{(A6)}$$

where the physically unacceptable solution has been discarded. Dividing both sides of (A5) by [L] and substituting (A6) on the right side, one obtains eq 2 after some simplification.

Registry No. 5′TTTTTGGTTACAAACTGTTCTTAA·TTAA-GAACAGTTTGTAACCAAAAA, 126898-28-0.

References

Beato, M. (1989) *Cell 56*, 335–344.

Berg, J. M. (1989) *Cell 57*, 1065–1068.

Bujalowski, W., & Lohman, T. M. (1987) *Biochemistry 26*, 3099–3106.

Cantor, C. R., & Schimmel, P. R. (1980) in *Biophysical Chemistry*, Part III, Freeman, San Francisco.

Carlstedt-Duke, J., Strömstedt, P.-E., Wrange, Ö., Bergman, T., Gustafsson, J.-Å., & Jörnvall, H. (1987) *Proc. Natl. Acad. Sci. U.S.A. 84*, 4437–4440.

Carlstedt-Duke, J., Strömstedt, P.-E., Dahlman, K., Rae, C., Berkenstam, A., Hapgood, J., Jörnvall, H., & Gustafsson, J.-Å. (1989) in *The Steroid/Thyroid Hormone Receptor Family and Gene Regulation* (Carlstedt-Duke, J., Eriksson, H., & Gustafsson, J.-Å., Eds.) pp 93–108, Birkhäuser Verlag, Basel, Switzerland.

Dahlman, K., Strömstedt, P.-E., Rae, C., Jörnvall, H., Flock, J.-I., Carlstedt-Duke, J., & Gustafsson, J.-Å. (1989) *J. Biol. Chem. 264*, 804–809.

deHaseth, P. L., Lohman, T. M., & Record, M. T. (1977) *Biochemistry 16*, 4783–4790.

Evans, R. M. (1988) *Science 240*, 889–895.

Freedman, L. P., Luisi, B. F., Korszum, Z. R., Basavappa, R., Sigler, P. B., & Yamamoto, K. R. (1988) *Nature 334*, 543–546.

Hagmar, P., Dahlman, K., Takahashi, M., Carlstedt-Duke, J., Gustafsson, J.-Å., & Nordén, B. (1989) *FEBS Lett. 253*, 28–31.

Mahler, H. R., Kline, B., & Mehrota, B. D. (1964) *J. Mol. Biol. 9*, 801-811.
McGhee, J. D., & von Hippel, P. H. (1974) *J. Mol. Biol. 86*, 469-489.
Miller, J., McLachlan, A. D., & Klug, A. (1985) *EMBO J. 4*, 1609-1614.
Payvar, F., & Wrange, Ö. (1983) in *Steroid Hormone Receptors: Structure and Function* (Eriksson, H., & Gustafsson, J.-Å., Eds.) pp 267-284, Elsevier, Amsterdam, The Netherlands.
Payvar, F., DeFranco, D., Firestone, G. L., Edgar, B., Wrange, Ö., Okret, S., Gustafsson, J.-Å., & Yamamoto, K. R. (1983) *Cell 35*, 381-392.
Press, W. H., Flannery, B. P., Teukolsky, S. A., & Vetterling, W. T. (1986) in *Numerical Recipes*, Chapter 14, Cambridge University Press, Cambridge, England.
Record, M. T., Lohman, T. M., & deHaseth, P. L. (1976) *J. Mol. Biol. 107*, 145-158.
Record, M. T., deHaseth, P. L., & Lohman, T. M. (1977) *Biochemistry 16*, 4791-4796.
Schwartz, G., & Watanabe, F. (1983) *J. Mol. Biol. 163*, 467-484.
Tsai, S. Y., Carlstedt-Duke, J., Weigel, N. L., Dahlman, K., Gustafsson, J.-Å., Tsai, M.-J., & O'Malley, B. W. (1988) *Cell 55*, 361-369.
Wrange, Ö., Eriksson, P., & Perlmann, T. (1989) *J. Biol. Chem. 264*, 5253-5259.
Yamamoto, K. R. (1985) *Annu. Rev. Genet. 19*, 209-252.

Peptide Models of Dynorphin A(1-17) Incorporating Minimally Homologous Substitutes for the Potential Amphiphilic β Strand in Residues 7-15†

John W. Taylor
Laboratory of Bioorganic Chemistry and Biochemistry, The Rockefeller University, New York, New York 10021
Received August 14, 1989; Revised Manuscript Received February 23, 1990

ABSTRACT: Two peptide models of dynorphin A(1-17) have been synthesized. These peptides incorporate a minimally homologous substitute sequence for residues 6-17, including alternating lysine and valine residues substituting for the potential amphiphilic β-strand structure in positions 7-15. Model 1 retains Pro^{10} from the native sequence, but model 2 does not. Compression isotherms of peptide monolayers at the air-water interface and CD spectra of peptide films adsorbed from aqueous solution onto siliconized quartz slides were evaluated by comparison to those of idealized amphiphilic α-helical, β-sheet, and disordered peptides. Dynorphin A(1-17) was mostly disordered, whereas β-endorphin was α helical. Dynorphin model 1 had properties similar to those of dynorphin A(1-17) at these interfaces, but model 2 formed strongly amphiphilic β sheets. In binding assays to μ-, δ-, and κ-opioid receptors in guinea pig brain membranes, model 1 reproduced the high potency and selectivity of dynorphin A(1-17) for κ receptors, and model 2 was only 3 times less potent and less selective for these receptors. Both peptide models retained the high, κ-selective agonist activity of dynorphin A(1-17) in guinea pig ileum assays, and like dynorphin A(1-17), model 1 had little activity in the rat vas deferens assay. In view of the minimal homology of the modeled dynorphin structures, these studies support current models of membrane-catalyzed opioid ligand-receptor interactions and suggest a role for the amphiphilic α-helical and β-strand structures in β-endorphin and dynorphin A(1-17), respectively, in this process.

Many biologically active peptides are highly flexible structures. They exist in multiple conformational states in aqueous solution that are profoundly affected by changes in the solution conditions, making it very difficult to identify functional conformations directly with any degree of confidence. Kaiser and Kezdy (1984) have suggested that the conformations adopted by these peptides, when they bind at the interfaces where they act will often be amphiphilic and stabilized by their environment. The identification of peptide segments having the potential to form amphiphilic α helices and β strands is relatively simple (Taylor & Kaiser, 1987), and helical structures of this type, in particular, appear to be very common. Furthermore, the functional significance of these amphiphilic helices has been determined in a number of cases, through the study of peptide models (Kaiser & Kezdy, 1984; Taylor & Kaiser, 1986). This approach involves the synthesis of analogues that are designed to retain the general characteristics of the proposed biologically active conformation in a nonhomologous structure. To the extent that the model peptides are able to reproduce the essential physicochemical and pharmacological properties of the native peptide while homology is minimized, evidence for the functional importance of the proposed conformation is obtained.

The naturally occurring opioid peptides appear to be an ideal system for study using nonhomologous models. These peptides share a common amino-terminal sequence of Tyr-Gly-Gly-Phe-Leu/Met, corresponding to the opioid peptides [Leu^5]- and [Met^5]enkephalin, that has highly specific interactions with its binding sites on μ-, δ-, and κ-opioid receptors (Hollt, 1983; Paterson et al., 1983). In contrast, the carboxy-terminal extensions of this sequence that are found in other opioid peptides appear to interact with receptors in a less specific fashion, judging by the effects of single amino acid residue deletions or substitutions, and yet these sequences have a profound effect on the pharmacological properties (Chavkin

†Support for this research was provided by USPHS Grant DA 04197. Dedicated to the memory of Professor Emil Thomas Kaiser.

0006-2960/90/0429-5364$02.50/0 © 1990 American Chemical Society